university of groningen

University Medical Center Groningen

University of Groningen

Spectral fiber dosimetry with beryllium oxide for quality assurance in hadron radiation therapy

Metzner, E.; Baeumer, C.; Behrends, C.; Debbih, A. Dammene; Doehler, D. D.; van Goethem, M. J.; van der Graaf, E. R.; Kahle, P.; Luehr, A.; Teichmann, T.

Published in:
Journal of Instrumentation

DOI:
10.1088/1748-0221/17/02/P02009

IMPORTANT NOTE: You are advised to consult the publisher's version (publisher's PDF) if you wish to cite from it. Please check the document version below.

Document Version
Publisher's PDF, also known as Version of record

Publication date:
2022

Link to publication in University of Groningen/UMCG research database

Citation for published version (APA):
Metzner, E., Baeumer, C., Behrends, C., Debbih, A. D., Doehler, D. D., van Goethem, M. J., van der Graaf, E. R., Kahle, P., Luehr, A., Teichmann, T., Timmermann, B., Weinberger, D., Werner, T., Wulff, J., & Kormoll, T. (2022). Spectral fiber dosimetry with beryllium oxide for quality assurance in hadron radiation therapy. *Journal of Instrumentation*, *17*(2), [02009]. https://doi.org/10.1088/1748-0221/17/02/P02009

Copyright
Other than for strictly personal use, it is not permitted to download or to forward/distribute the text or part of it without the consent of the author(s) and/or copyright holder(s), unless the work is under an open content license (like Creative Commons).

The publication may also be distributed here under the terms of Article 25fa of the Dutch Copyright Act, indicated by the “Taverne” license. More information can be found on the University of Groningen website: https://www.rug.nl/library/open-access/self-archiving-pure/taverne-amendment.

Take-down policy
If you believe that this document breaches copyright please contact us providing details, and we will remove access to the work immediately and investigate your claim.

Downloaded from the University of Groningen/UMCG research database (Pure): http://www.rug.nl/research/portal. For technical reasons the number of authors shown on this cover page is limited to 10 maximum.

Download date: 12-10-2022

Journal of Instrumentation

SISSA

PAPER

Spectral fiber dosimetry with beryllium oxide for quality assurance in hadron radiation therapy

To cite this article: E. Metzner *et al* 2022 *JINST* **17** P02009

View the article online for updates and enhancements.

You may also like

- Radioluminescence in biomedicine: physics, applications, and models
Justin S Klein, Conroy Sun and Guillem Pratx
- Radioluminescence by synchrotron radiation with lower energy than the Cherenkov light threshold in water
Yoshiyuki Hirano, Masataka Komori, Daichi Onoda et al.
- Optical dosimetry for ionizing radiation fields by infrared radioluminescence
T Shikama, K Toh, S Nagata et al.

IOP ebooks™

Bringing together innovative digital publishing with leading authors from the global scientific community.

Start exploring the collection–download the first chapter of every title for free.

This content was downloaded from IP address 129.125.135.122 on 09/05/2022 at 13:20

Published by IOP Publishing for Sissa Medialab

Received: *September 15, 2021*
Revised: *October 19, 2021*
Accepted: *November 1, 2021*
Published: *February 4, 2022*

Spectral fiber dosimetry with beryllium oxide for quality assurance in hadron radiation therapy

E. Metzner,[a,*] **C. Bäumer,**[b,c,d,e] **C. Behrends,**[b,c,d] **A. Dammene Debbih,**[b,c,f] **D.D. Döhler,**[a] **M.J. van Goethem,**[g] **E.R. van der Graaf,**[g] **P. Kahle,**[a] **A. Lühr,**[d] **T. Teichmann,**[a,1] **B. Timmermann,**[b,c,e,h,i] **D. Weinberger,**[j] **T. Werner,**[a] **J. Wulff**[b,c] **and T. Kormoll**[a,j]

[a] *Institute for Nuclear and Particle Physics, TU Dresden, Zellescher Weg 19, 01069 Dresden, Germany*
[b] *West German Proton Therapy Centre Essen (WPE), University Hospital Essen, Hufelandstr. 55, 45147 Essen, Germany*
[c] *West German Cancer Centre (WTZ), University Hospital Essen, Hufelandstr. 55, 45147 Essen, Germany*
[d] *Department of Physics, TU Dortmund University, Otto-Hahn-Str. 4, 44227 Dortmund, Germany*
[e] *Deutsches Konsortium für Translationale Krebsforschung (DKTK), Im Neuenheimer Feld 280, 69120 Heidelberg, Germany*
[f] *Hochschule Hamm-Lippstadt, Marker Allee 76–78, 59063 Hamm, Germany*
[g] *Department of Radiation Oncology, University Medical Centre Groningen, University of Groningen, Hanzeplein 1, 9713 GZ Groningen, the Netherlands*
[h] *Faculty of Medicine, University of Duisburg-Essen, Hufelandstr. 55, 45147 Essen, Germany*
[i] *Department of Particle Therapy, University Hospital Essen, Hufelandstr. 55, 45147 Essen, Germany*
[j] *Serious Dynamics GbR, Altkaditz 5a, 01139 Dresden, Germany*

E-mail: elena.metzner@tu-dresden.de

Abstract: Using the radioluminescence light of solid state probes coupled to long and flexible fibers for dosimetry in radiotherapy offers many advantages in terms of probe size, robustness and cost efficiency. However, especially in hadron fields, radioluminophores exhibit quenching effects dependent on the linear energy transfer. This work describes the discovery of a spectral shift in the radioluminescence light of beryllium oxide in dependence on the residual range at therapeutic proton

[1] Now at: Fraunhofer FEP, Winterbergstraße 28, 01277 Dresden, Germany.
[*] Corresponding author.

© 2022 IOP Publishing Ltd and Sissa Medialab
https://doi.org/10.1088/1748-0221/17/02/P02009

2022 JINST 17 P02009

energies. A spectrally resolving measurement setup has been developed and tested in scanned proton fields. It is shown that such a system can not only quantitatively reconstruct the dose, but might also give information on the residual proton range at the point of measurement.

KEYWORDS: Dosimetry concepts and apparatus; Instrumentation for hadron therapy; Scintillators and scintillating fibres and light guides; Solid state detectors

2022 JINST 17 P02009

Contents

2022 JINST 17 P02009

1 Introduction

Percutaneous cancer irradiation, especially with hadrons, requires accurate dosimetry with high spatial resolution, e.g. for efficient quality assurance procedures. Ionization chambers are routinely used for absolute and relative dosimetry such as the determination of depth-dose curves. However, as gas detectors they have need for large sensitive volumes to assure an adequate signal to noise ratio in dose measurements. This leads to crucial limitations in spatial resolution and required corrections in small radiation fields.

Alternative systems like synthetic diamond detectors [1] or diode detectors [2] are providing accurate dose readings at a very small size. However, these systems rely on the transmission of relatively weak electrical signals out of the irradiation room. The electrical nature of the transmission further compromises the compatibility with magnetic resonance imaging (MRI) systems which are being integrated into the irradiation facility [3, 4].

A solution could be the use of radioluminescent materials and their sensitivity to ionizing radiation. Radioluminescent probes, where a small luminophore is placed on the tip of a long and flexible light guide, can yield accurate dose readings with a very robust signal transmission [5–8]. The signal output allows for very small sensitive volumes ($< 1\,\mathrm{mm}^3$) and therefore good spatial

resolution. The probes are potentially highly cost effective and could be used in in-vivo experiments as disposable items. Furthermore, the use of silica fibers as light guides renders robust optical signal transmission that is not sensitive to electromagnetic fields and could be integrated in an MRI environment [9, 10].

However, in hadron fields, most solid state radioluminophores experience a decrease in signal strength in dependence on the linear energy transfer (LET) and thereby an underestimation of dose, especially in the relevant Bragg peak region.

Beryllium oxide (BeO) is a ceramic, radioluminescent material with a nearly tissue equivalent effective atomic number $Z_{\text{eff}} \approx 7.2$ and therefore suited for dosimetry applications [11]. It shows a linear dose response [7, 12] in both radioluminescence (RL) and optically stimulated luminescence (OSL) emission and has already been successfully tested and implemented for dosimetric measurements in photon fields [7, 12–14]. In proton beams, the luminescence experiences quenching effects in regions of high LET which leads to dose underestimation especially in the Bragg peak. In previous experiments, it was possible to correct the quenching effects in proton fields using a combination of the RL and OSL signals [5]. This required however a second reading using optical stimulation after the irradiation. During measurements with a real-time OSL setup, the results suggested a change of the RL spectrum in different LET radiation fields [15]. This prompted a more thorough investigation into the spectral composition of radioluminescence in BeO.

During proton irradiation at the AGOR cyclotron in Groningen, Netherlands, it was discovered that the spectral composition of radioluminescence in BeO is dependent on the residual range of the protons, and presumably the LET. The results of this experiment gave inspiration to the development of a new measuring system. This system was designed to exploit this effect for a dose correction in proton fields without the need of post irradiation measurements.

In this work, these spectrally resolved measurements in the proton field of the research cyclotron AGOR are presented. Based on the observations in that research environment, an optical setup for dosimetry measurements has been developed and tested in the clinical proton radiotherapy facility Westdeutsches Protonentherapiezentrum Essen (WPE) in Essen, Germany. It will be shown that this setup is not only able to accurately measure the delivered dose, but can also give information on the residual beam range at the position of measurement. Additionally, with the information about the applied spot pattern during a pencil beam scanning (PBS) procedure, it was also possible to extract the lateral beam profile due to the high time resolution of the measured RL light signal. This enhanced dosimetry can potentially simplify quality assurance routines.

2 Methods and materials

2.1 Emission spectra measurements at AGOR

At the superconducting AGOR cyclotron in Groningen, the Netherlands, irradiation experiments of a BeO probe with protons were done to investigate the RL emission spectra of BeO in different parts of the Bragg curve.

2.1.1 Experimental setup and data acquisition

Irradiations were done with a fixed proton energy of 190 MeV. The accelerated protons went through a single scattering setup resulting in a 30 mm beam diameter and a mean range of 222 mm in water.

2022 JINST 17 P02009

A small volume of BeO was coupled to a 2 m long SiO_2 fiber by THORLABS with a core diameter of 1 mm. The BeO probe was cylindric with a diameter and height of 1 mm, respectively, resulting in a sensitive volume of 0.79 mm^3. The BeO probe was glued to the glass fiber with UV-translucent epoxy resin and the entire fiber probe head enclosed in black epoxy resin for light-tightness. Figure 1 shows the almost identical[1] fiber probe head manufactured for the experiments at WPE. The finished probe was pre-irradiated in photon fields with a total dose > 300 Gy. The measuring signal, emitted in the probe head, was transmitted through the fiber to a grating spectrometer (SI Spectroscopy Instruments, SP150). The grating spectrometer allows a spectral decomposition of the signal by filtering for one distinct, selectable wavelength. The signal part of the requested wavelength was then forwarded to a single photon counting head (SPCH) (Hamamatsu Photonics, H10682-210) for the subsequent analysis. A schematic sketch of the measuring system can be seen in figure 2.

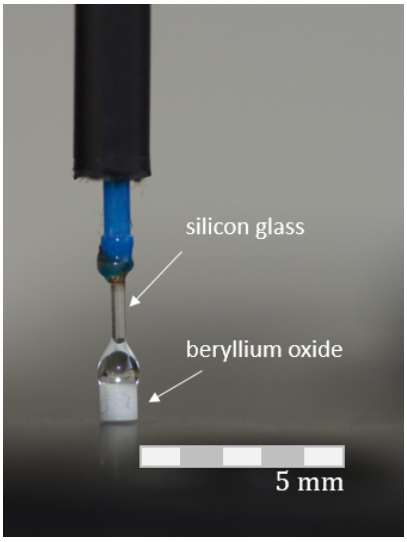

Figure 1. Close-up of the exposed fiber probe head with the radioluminescent beryllium oxide and silicon glass fiber core visible.

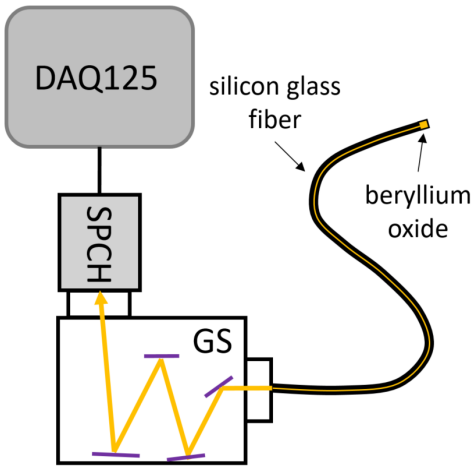

Figure 2. Sketch of the measuring system for the experiments at AGOR. The light emitted in beryllium oxide is transmitted through a silicon glass fiber and directed at a grating spectrometer (GS), which forwards the signal corresponding to a selected wavelength. The signal is read out by a single photon counting head (SPCH) and a digital read-out unit (DAQ125).

For each detected photon, the SPCH releases a short voltage signal pulse that is then sampled by a 125 MHz read-out unit (DAQ125 by Serious Dynamics) and analyzed with an integrated FPGA. The gained data contains information about the pulse shape and time stamp (in relation to the beginning of measurement) for each event. Thus, it was possible to determine the event count rate proportional to the emission intensity for the selected wavelength. By taking the recorded pulse shape into account, it was possible to identify pile-up events and correct the event rate accordingly.

2.1.2 Measurement program

The sensitive BeO probe was placed in a water tank on a movable adapter and navigated to the requested measuring depths for irradiation. The electronic readout unit was positioned as far out of the beam line as possible and shielded with polyethylene and lead bricks.

[1]The fibers prepared for the two experiments differ solely in fiber length and diameter of the silicon glass core.

2022 JINST 17 P02009

Two measuring campaigns for different probe positions were performed. The first measuring point was in 40 mm depth (plateau of the Bragg curve), and the second one at 200 mm (rising region of the Bragg curve) in the water tank. In each depth, 22 irradiations for different spectrometer settings were done and the event count rates over a detection time of 600 s were recorded. The wavelengths were selected within the range from 275 nm to 425 nm.

2.1.3 Results of spectrally resolved measurements at AGOR

The results of the spectral measurements at two different depths in the water tank are shown in figure 3. Light with a wavelength below 270 nm could not be measured due to the limited spectral sensitivity of the SPCH. Both emission spectra show a structure of two broad maxima at $\lambda \approx 315$ nm and $\lambda \approx 375$ nm, with a local minimum at $\lambda \approx 340$ nm. These observations are in agreement with RL spectra from photon stimulation previously measured in [16].

However, the spectral emission intensity shows changes depending on the residual range of the protons. Aside from a higher total emission intensity for the measurement in the deeper position, the outstanding effect is the different ratio between the two maxima amplitudes. The clear prominence of the second maximum ($\lambda = 375$ nm) is no longer the case in a measuring position deeper in the water tank, where the residual proton range is shorter and the LET is higher.

A measuring system able to record the ratio between the two emission maxima would therefore be able to give information about the residual proton range of the beam. This motivated the use of a dichroic beam splitter with a separation wavelength in the area of the minimum. The developed measuring system is explained below in section 2.2.

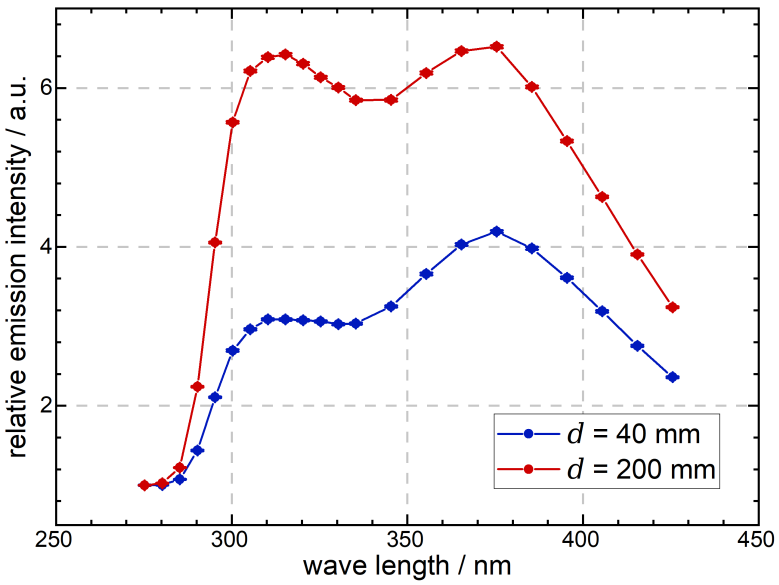

Figure 3. RL emission spectrum of BeO measured in a water tank at the proton cyclotron AGOR with a grating spectrometer. For both positions at depths $d = 40$ mm and $d = 200$ mm, there are two broad emission maxima with a local minimum around $\lambda = 340$ nm. The ratio of the maxima amplitudes differs for measurements taken in different depths.

2022 JINST 17 P02009

2.2 Depth-dose measurements at WPE

The results from the spectrally resolved measurements at AGOR inspired a new method of dose measurements with BeO. A measuring system including a dichroic beam splitter was developed and the method tested on depth-dose measurements in a clinical proton beam at WPE in Essen.

2.2.1 Measuring System for spectral fiber dosimetry

Figure 4 shows a schematic sketch of the measurement system for the experiments at WPE.

A detection probe consisting of a BeO tipped silicon glass fiber similar to the one used in the AGOR experiment was used. It was pre-irradiated with a total dose > 100 Gy during preceding experiments in the clinical proton beam. The fiber used for this experiment was longer and slimmer than the one at AGOR in order to reduce the stem effect of radioluminescence and Cherenkov light in the fiber as well as direct ionization in the SPCHs. In this case, the fiber was 5 m long with a core diameter of 400 µm while the BeO volume had the same dimensions as before. The exposed fiber probe head is shown in figure 1.

Instead of a grating spectrometer, the signal of the fiber was directed at a dichroic beam splitter (FF347-Di01-25x36, Semrock Inc.). Its transmission edge is located at $\lambda_c = 347$ nm and therefore separates the signal in the local minimum between the two emission maxima discovered during the AGOR experiment (section 2.1.3). The respectively reflected and transmitted light beams are consequently read out by two identical SPCHs (µPMT H12406 series, Hamamatsu), resulting in two recorded signals: the R signal (reflected light, $\lambda < \lambda_c$) and the T signal (transmitted light, $\lambda > \lambda_c$). The detection unit DAQ125 already used in the AGOR experiments records the produced voltage pulses from both SPCHs simultaneously and with correlated time stamps. A measurement of a single irradiation therefore gives the event count rates from the R, T and the total $M = R + T$ signal.

2.2.2 Experimental setup and beam delivery

Experiments were carried out at WPE in Essen, Germany, at a clinical proton therapy system with an isochronous cyclotron (Proteus®PLUS, IBA) which accelerates protons to an energy of 226.7 MeV. For the experiments, the proton beam energy was reduced in the energy-selection system downstream of the cyclotron to 100 MeV, corresponding to a mean proton range $R_{\mathrm{CSDA}} = 77.3$ mm in water [17]. The beam delivery system was operated in pencil beam scanning (PBS) mode, where the proton beam is guided over the target volume with scanning magnets in discrete steps. Therefore, the scanned field is subdivided in distinct irradiation points (PBS spots). The radiation field had an area of 30 mm × 30 mm with a substructure of 13 × 13 = 169 PBS spots per delivered field with a respective distance of 2.5 mm between the targeted positions of the beam center. A schematic sketch of the radiation area and the positioning of the measuring fiber is shown in figure 5. The order of irradiation went in horizontal lines from top to bottom and left to right. The intensity was the same for each spot resulting in an inhomogeneous dose distribution but well suitable to study the probe response to distinct spots.

Measurements were done with a MP3-XS phantom by PTW with a modified entrance window of 1.16 mm water equivalent thickness. The phantom allows positioning of a detector in 3 dimensions by means of linear axis. The BeO fiber was inserted from above, perpendicularly to the beam line, and positioned with the BeO cylinder in the iso center of the field. The fiber was connected to

2022 JINST 17 P02009

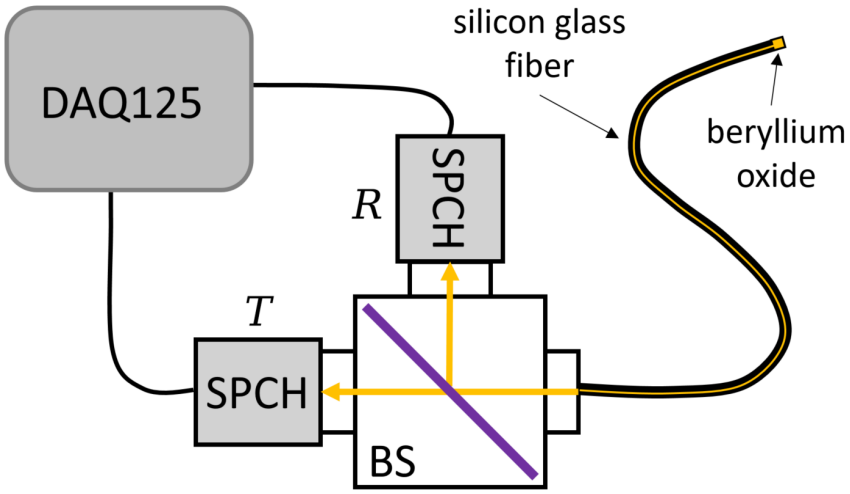

Figure 4. Sketch of the measuring system for the experiments at WPE. The light emitted in beryllium oxide is transmitted through a silicon glass fiber and spectrally separated into two parts R and T by a dichroic beam splitter (BS). The two signals are read out by two single photon counting heads (SPCHs) and a digital read-out unit (DAQ125).

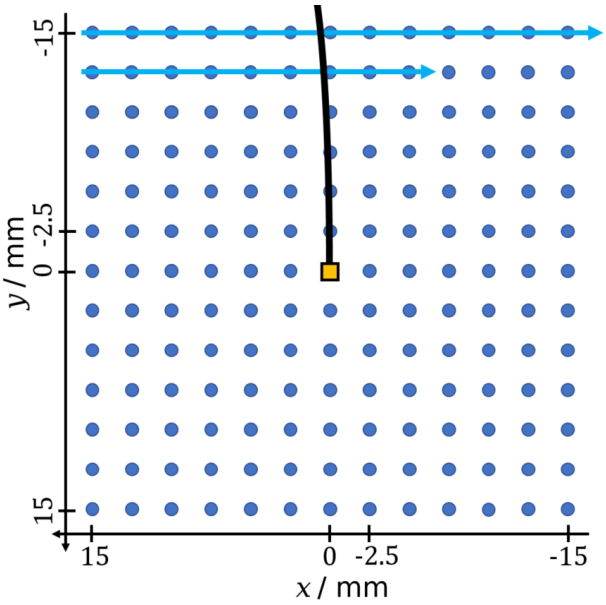

Figure 5. Sketch of the applied radiation field at WPE structured into 169 PBS irradiation spots. The spots were scanned in horizontal lines from left to right and top to bottom. The measuring fiber (black) was inserted from the top with the BeO cylinder (orange) positioned in the iso center of the field.

the electronic read-out unit positioned appr. 3 m away from the iso center of the field in a slightly upstream position.

As reference, the depth-dose curve measurements were repeated with an Advanced Markus Chamber (AMC) (type 34045, PTW). It was positioned so that the center of the gas cavity was in the iso center of the radiation field.

2022 JINST 17 P02009

2.2.3 Measurement program

Measurements at 28 measuring depths were done with the BeO fiber setup and a reference measurement with the AMC was performed. The respective detection system was moved to the measuring depths in the phantom using a mounting system connected to the mechanic moving system of the phantom, which provides 3D mobility along three linear axes and is remotely controllable. Within the Bragg peak region measurements were taken with a step resolution of 1 mm. The depth range included the entirety of the Bragg peak, ranging from appr. 30 mm water equivalent depth (WED) to appr. 81 mm WED. Due to the different detection systems, slight deviations in the effective point of measurement were taken into account by determining the water equivalent thickness of the entrance and thus reference point of the detectors (explained below). The initial setup of the detectors within the phantom, defining the null-position of the measurements, was tuned with the x-ray based patient positioning system. The reference points the position was defined for were the center of the BeO cylinder and the center of the outer front wall of the AMC.

2.2.4 Dose correction

In low LET regions, the light emission intensity of BeO is proportional to the locally absorbed dose. The experimental setup enables the separation of the RL light into two parts: R and T, which makes for three possible signals when including the full light emission $M = R + T$. All three show this dose proportionality and can be used to determine the dose:

$$D_{\mathrm{BeO},X} = D(X)\,; \qquad X \in \{M,\, R,\, T\} \tag{2.1}$$

Likewise, all three signals, when taken on their own, show an underestimation of dose in high LET regions.

The amount of dose underestimation due to quenching effects is dependent on the LET, and consequentially the residual proton range $R_{\mathrm{res}} = R_{\mathrm{CSDA}} - \mathrm{WED}$. It is quantifiable by the ratio f of the dose $D_{\mathrm{BeO},X}$ measured with BeO and the reference $D_{\mathrm{ref.}}$, in this case measured with the AMC:

$$f = \frac{D_{\mathrm{ref.}}}{D_{\mathrm{BeO},X}} \tag{2.2}$$

The two signal parts R and T correspond to the left and right side of the spectrum, separated in its local minimum observed in section 2.1.3. They therefore give information about the integrated intensity of the two emission maxima. The ratio γ of the two

$$\gamma = \frac{R}{T} \tag{2.3}$$

is dependent on R_{res} as well.

It will be shown that this results in an exponential dependency of $f(R_{\mathrm{res}})$ on $\gamma(R_{\mathrm{res}})$. Therefore, the correction function $f_{\mathrm{corr.}}(\gamma)$ can be obtained by analyzing a depth-dose measurement of the Bragg curve, where the protons undergo a continuous energy loss and change in LET. The corrected dose of the BeO measurement is then

$$D_{\mathrm{corr.}} = f_{\mathrm{corr.}}(\gamma) \cdot D_{\mathrm{BeO},X} \tag{2.4}$$

and can be determined for every measurement.

2022 JINST 17 P02009

The exact WED of each measuring point with regards to the effective point of measurement of both measuring systems in water has to be determined for the data analysis. For this purpose, the known stopping power (taken from stopping power calculations in [17] and [18]) and mass densities of the involved materials were taken into consideration. For example, the optical fiber setup was positioned using the distance between the inner water tank wall and the center of the BeO cylinder. To calculate the effective point of measurement, the water equivalent thickness of: the water tank wall, its distance to the fiber edge, the epoxy resin around the BeO, and the BeO to the cylinder center were determined with stopping power and mass density corrections where available.

3 Results

3.1 Beam profile and radiation field at WPE

Figure 6 shows the event times histograms of the R and T signal during a single irradiation, meaning one complete scanning of the 30 mm × 30 mm radiation field (figure 5).

The ratio of the two emission maxima can be perceived by the different event rates per readout channel and quantified by the number of events counted respectively. Both signals follow the same structure of multiple peaks. In figure 6a one can verify that the emission of light happens only during and with very small event rates before irradiation, corresponding to the SPCHs' dark count rate (pre-measured in a 60 min measurement, stable around 3 counts/s to 5 counts/s). After irradiation there is however a weak afterglow of slightly higher event rates. This could be attributed to both the de-excitation of particles in the water tank and an effect from the BeO.

The multiple peak structure in the event times histogram can be explained by irradiation via PBS. In figure 6a, the exterior structure consisting of 13 large peaks is created due to the scanning of irradiation spots in 13 horizontal lines. With smaller binning, it is also possible to see the interior structure of the individual irradiation spots in figure 6b, where each of the 13 larger peaks consists of 13 smaller peaks. All 169 irradiation spots are distinguishable in the event time histogram.

With the BeO in the iso center of the field, the relative distance between the proton beam and the sensitive volume changes with each spot scanned by the PBS system. This causes the event rates to increase and then decrease both in the exterior structure of horizontal lines (beam travels from top to bottom) and the interior structure within one horizontal line (beam travels from left to right).

In combination with the known PBS spot grid pattern and position of the BeO, it is possible to derive the single pencil beam profile at measuring depth from the data acquired by a single measurement. Assuming that the proton beam profile does not significantly change while scanning the radiation area, moving the beam relative to the BeO is virtually the same as moving the BeO probe relative to a stationary beam. With the BeO in the iso center of the radiation field, the event counts per PBS spot give the proton beam profile (double mirrored along the diagonals through the BeO position).

Therefore the measuring time is divided into 169 time intervals for all single-irradiation-peaks and the corresponding PBS spot is determined from the PBS grid pattern (by scanning order). For each spot, the dark-count-corrected number of events is calculated.

2022 JINST 17 P02009

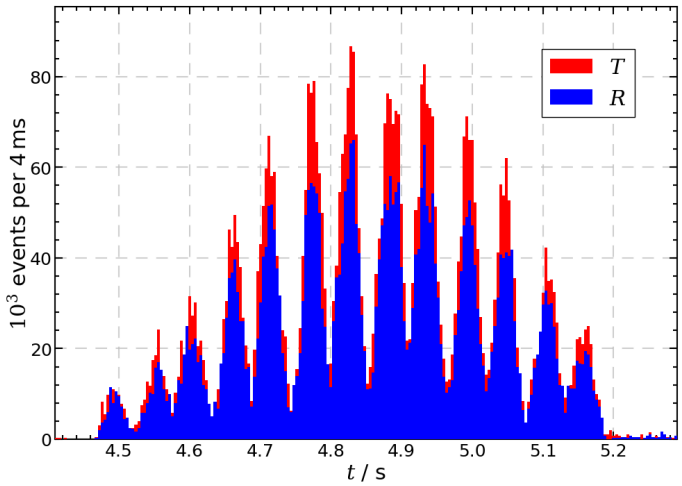

(a) Full irradiation time, bin width of 4 ms. Exterior peak structure of horizontal PBS spot lines.

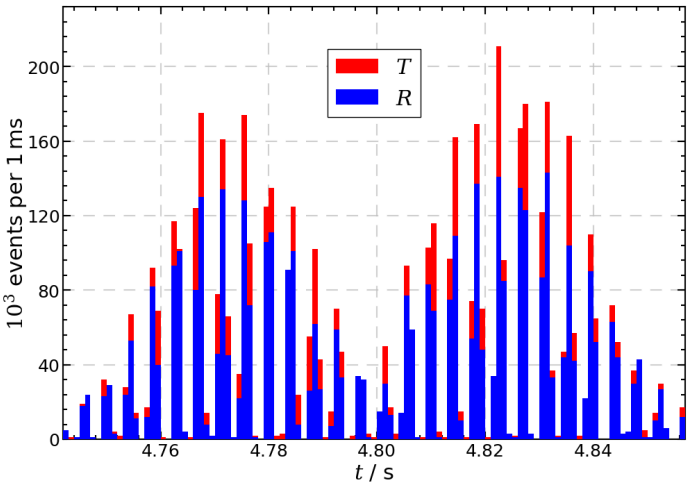

(b) 6th and 7th peak in figure 6a, bin width of 1 ms. Interior peak structure of individual PBS spots.

Figure 6. Event times histograms of a single irradiation measurement with BeO in WED = 64.77 mm, shown in number of events per time bin. The events of the two signal parts R and T are shown separately and showcase the different emission intensities. The multiple peak structure stems from irradiation via pencil beam scanning, all 169 PBS spots are distinguishable in the data.

In figure 7 the resulting pencil beam profile is shown as a standard contour plot. A 2-dimensional Gaussian fit was applied to the result with the standard deviations:

$$\sigma_x = (8.25 \pm 0.22)\ \text{mm}$$
$$\sigma_y = (8.16 \pm 0.20)\ \text{mm}$$

The width of the pencil beam profile indicates that overlapping occurs while scanning the PBS spots, which have respective distances of 2.5 mm.

2022 JINST 17 P02009

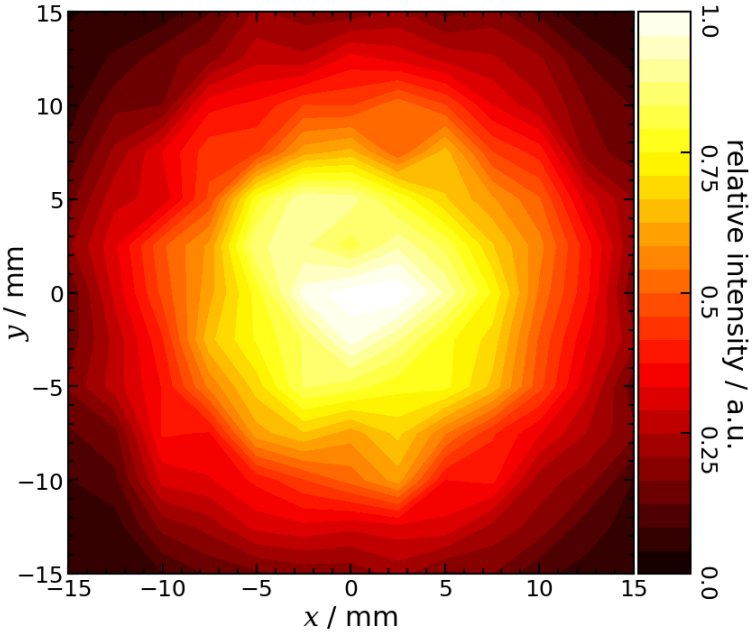

Figure 7. Lateral proton pencil beam profile determined from a single measurement at WED ≈ 30 mm. The profile is taken from 169 measuring points (PBS spots) at different relative distances (due to PBS) between the BeO and proton beam. The profile is scaled to the maximum intensity.

3.2 Depth-dose curves at WPE

The depth-dose curves were analyzed in arbitrary units. The reference data was taken from the AMC data points fitted with a Bortfeld function [19]. The curves were scaled to the plateau before the Bragg peak at WED = 40 mm for comparison using linear extrapolation between discrete measuring points.

For each measuring point taken with the BeO setup, the relative dose is given by the total amount of events detected during a full PBS process at the corresponding measuring depth, corrected with the SPCH's dark count. All three signal possibilities R, T, and $M = R + T$ show similar behavior throughout the Bragg peak, yet the divergence from the reference is the smallest for the reflected signal R. To minimize the dose correction needed, it makes sense to use this signal to determine the dose $D_{\mathrm{BeO},R} = D(R)$ and make use of the information of transmitted light T only via $\gamma = R/T$.

The dose underestimation f taken by comparing the BeO measurement with the reference can be seen in figure 8. As expected due to previous dosimetry measurements with BeO [5], the emission signal follows the deposited dose in the first half of the Bragg peak ($f \approx 1$) before starting to diverge around WED ≈ 76 mm. Here, f starts to greatly increase until reaching its maximum at WED ≈ 81 mm.

The dependence of the reflected and transmitted signal ratio $\gamma = R/T$ on different WED is also shown in figure 8. It clearly shows a dependency of γ on the residual proton range $R_{\mathrm{res}} = R_{\mathrm{CSDA}} - \mathrm{WED}$, confirming the assumptions of this development depending on the LET of the protons. The sensitivity of γ to R_{res} becomes greater in the region of interest (the Bragg peak) but abruptly changes its rising behavior behind WED ≈ 79 mm. The point of behavioral change is appr. 2 mm further upstream of where the dose underestimation starts to decrease again. This point corresponds to appr. R_{70} of the reference measurement, which is $R_{70} = 78.99$ mm.

2022 JINST 17 P02009

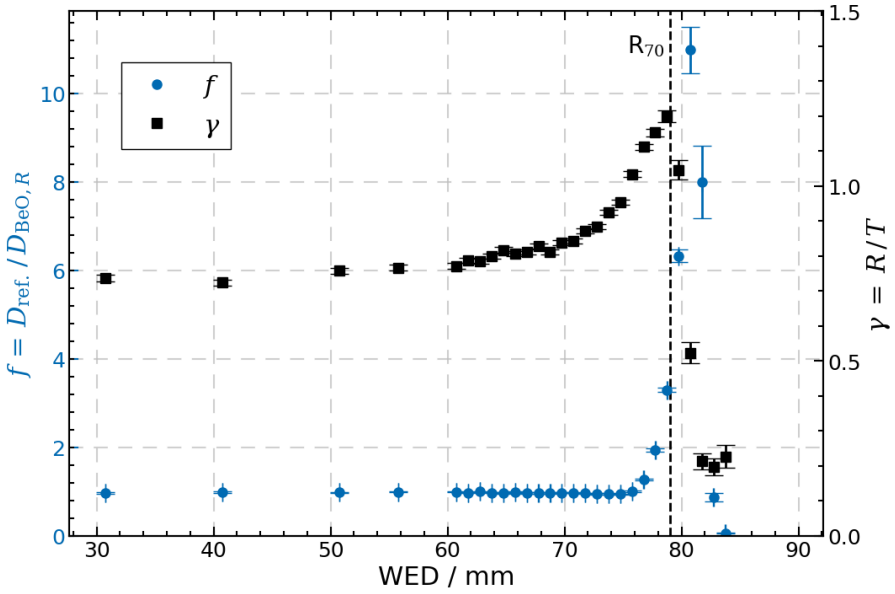

Figure 8. The dose underestimation f and signal ratio γ over the WED of the corresponding BeO measurement. f is relatively constant at $f \approx 1$ and starts to increase at WED ≈ 76 mm. γ increases up to WED $\approx R_{70}$ and abruptly decreases downstream. The behavioral change in γ happens approx. 2 mm upstream of where f reaches its maximum at WED ≈ 81 mm.

The dependency of f on γ can be seen in figure 9. It increases exponentially until the maximum of γ is reached at WED $\approx R_{70}$. The measuring points taken at depths WED $> R_{70}$ do not show the same dependency and had to be excluded from analysis. Only the measuring points with WED $\leq R_{70}$ were fitted with an exponential fit function

$$f_{\text{corr.}}(\gamma) = f_0 + a \cdot \exp(b \cdot \gamma)$$

to determine the correction function $f_{\text{corr.}}$. The resulting parameters with their uncertainties of one standard deviation are:

$$\begin{aligned} f_0 &= 0.972 \pm 0.007 \\ a &= 3.8 \cdot 10^{-11} \pm 2.9 \cdot 10^{-11} \\ b &= 20.7 \pm 0.6 \end{aligned}$$

The relatively high uncertainties likely stem from the small number of measuring points in the relevant region $1.0 \leq \gamma \leq 1.2$, corresponding to the measuring points at 76 mm $\leq$ WED $\leq R_{70}$. This may cause problems with the chosen fitting method of non-linear least squares and result in the overestimation[2] of parameter uncertainties. Due to the obviously good fit of the parameter values themselves, the correction function $f_{\text{corr.}}$ has been deemed acceptable for the purpose of introducing this measuring method.

The excluded measuring points downstream of R_{70} show decreased γ values so that $f_{\text{corr.}}(\gamma)$ does not match the actual dose underestimation f. However, when applying the dose correction

[2]A visualization of the effect of the given uncertainties on the course of $f_{\text{corr.}}$ shows a clear disconnect from the data, suggesting that the uncertainties are indeed overestimated by the fitting method.

2022 JINST 17 P02009

function after eq. (2.4) it becomes clear that values of $f_{\text{corr.}}(\gamma) \approx 1$ have no effect on the dose measurement. Since this is the case for all measuring points downstream of R_{70}, it was decided that the dose correction taken from $f_{\text{corr.}}(\gamma)$ is still applicable in this region, but does not improve upon the dose underestimation.

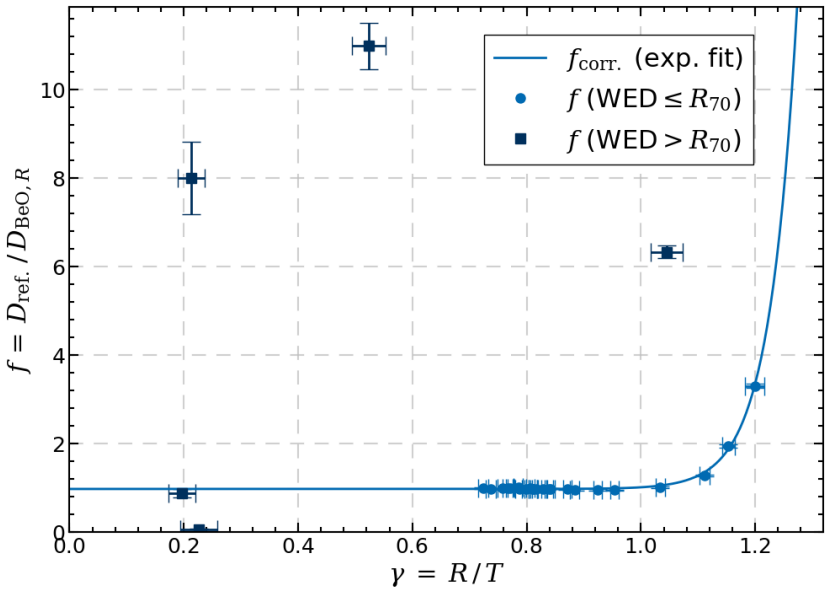

Figure 9. The dose underestimation f over the signal γ for all measurements with BeO. f shows an exponential dependency for measurements taken in WEDs up to R_{70} of the beam. The remaining measuring points are excluded from the exponential fit yielding $f_{\text{corr.}}$.

The resulting depth-dose curves are shown in figure 10 in arbitrary units. The black (circle) points show the data points taken with the BeO setup before a dose correction. Here, the abrupt onset of dose underestimation in the Bragg peak can be seen clearly. The blue (triangle) data points show the beryllium oxide measurement data after the application of the dose correction function. It shows the success of this method in the height of the Bragg peak, where the largest part of dose is deposited. Due to the γ factor discrepancy mentioned above, a continued dose underestimation can be observed in the tail of the Bragg peak. The dose correction shows accuracy in the area of interest up to R_{70}.

4 Discussion

It was shown that spectral fiber dosimetry with beryllium oxide gives a method to determine a correction function for the otherwise seen dose underestimation in the Bragg peak. This method is applicable in the height of the Bragg peak where the better part of dose application occurs.

To verify that the application of the dose correction function translates to accurate dosimetry measurements, a measurement with the same setup in a known radiation field would suffice. Unfortunately, due to circumstances unrelated to the experiments itself, the fiber probe used for the measurements at WPE was damaged and could not be used for verification. However, previous

2022 JINST 17 P02009

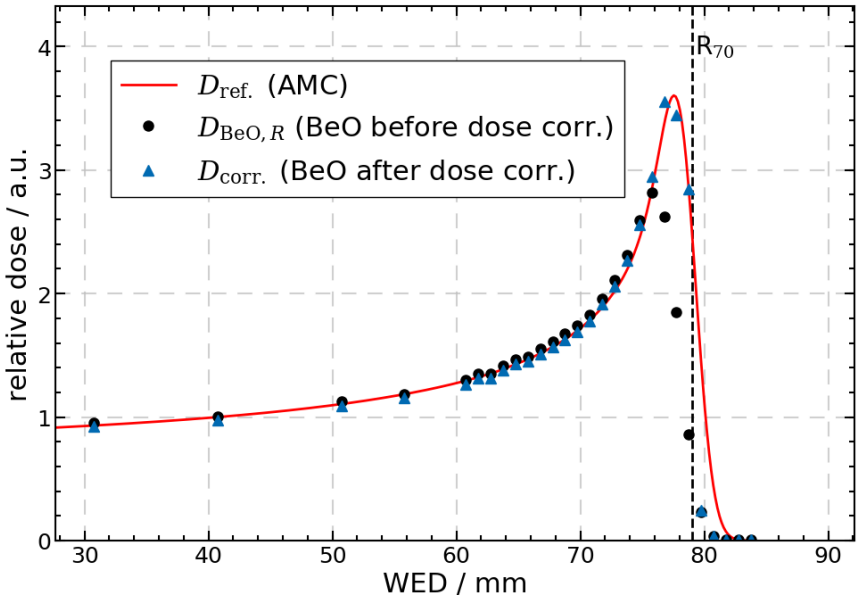

Figure 10. Depth-dose measurements in the Bragg curve, scaled to WED = 40 mm. The reference data $D_{\text{ref.}}$ was taken with an Advanced Markus Chamber (AMC) and fitted with a Bortfeld curve [19]. The dose from the BeO measurement $D_{\text{BeO},R}$ shows a dose underestimation in the Bragg peak. After the application of the dose correction function, $D_{\text{corr.}}$ follows the reference data up to R_{70}.

experiments with a similar, preliminary setup included a successful verification measurement and highly suggest that this method can result in accurate dosimetry.

A potential application in clinical environments would require such verification measurements as well as a more detailed investigation of the behavior in the Bragg peak. Finer spacing of the measuring points in the region of interest, where the onset of dose underestimation starts, would most likely improve the determination of $f_{\text{corr.}}(\gamma)$ and its uncertainty by improving the least squares fitting process. The continued dose underestimation downstream of the Bragg peak can be quantified and plays a relatively small role compared to the total amount of dose. The present results strongly suggest that the translation of this measuring method to clinical applications is possible with the corresponding precision in measurements.

The event times histograms shown in figure 6 can be used to analyze the response of the BeO detector during a complete PBS irradiation. Aside from the main peak structure already discussed above, the histograms show two additional effects best seen in figure 6a. First, the detected event count rates are higher during the second half of irradiation, causing a slight asymmetry. Additionally, a second interesting effect can be observed when comparing the amount of reflected (R) and transmitted (T) light (and consequently γ) in the first and second half of irradiation. In the beginning, R and T are almost equal and the difference builds up during irradiation. There are multiple reasons for a measurement with a moving proton beam to show these two effects. The first one is the stem effect of the fiber, mainly caused by direct ionization and Cherenkov light in its silicon glass core [20, 21]. Since the fiber reaches only half-way into the phantom, coming from above, its interaction with the pencil beam should be higher during the irradiation of PBS spots in the top half of the radiation area. The light due to stem effect is mostly blue and would therefore

2022 JINST 17 P02009

also cause a change in γ. However, with the beam scanning from top to bottom, this would be expected to express itself as an asymmetry with heightened event count rates during the first half of irradiation, not the second half. A second possibility would be an asymmetric pencil beam profile with higher dose rates on one side, causing more dose deposition during one half of the PBS process when that side is directed towards the probe. If this asymmetry were caused by deflected protons, the consequently changed residual proton range might be linked to the change in γ. The third would be the existence of excitation states in BeO with longer de-excitation half times in the range of ms. A partial signal delay might be visible as the observed asymmetry even if only a small portion of the full signal were affected. If these ms-lasting excitation states favored one side of the RL spectrum, γ would obviously change during irradiation, but when waiting long enough for de-excitation to occur it should have no effect on the measurement as a whole.

While the measurements at AGOR show that the emission spectrum of BeO depends on the residual range of the protons, the underlying effect is still unknown. Therefore, the behavior of the indicator γ is also not well understood. The abrupt change in behavior of the γ factor downstream of $R_{70} = 78.99\,\mathrm{mm}$ might be due to the substantial change of the radiation field in this region. Here, the particle composition and the mechanism of energy deposition becomes more complex due to effects like range and energy straggling. This explanation is supported by the fact that the effect is seen shortly downstream of the nominal range of the primary protons $R_{\mathrm{CSDA}} = 77.3\,\mathrm{mm}$ from continuous slowing down approximation. However, this possible explanation is only speculative. In order to further understand the behavior of BeO in high LET environments, irradiation with heavier particles could provide valuable information.

5 Conclusion

The spectrum of radioluminescence light in BeO was investigated in a research proton beam. It shows two emission maxima with varying amplitudes, where the ratio of the maxima amplitudes depends on the residual proton range. This effect was utilized in a new method of spectral fiber dosimetry measurements using a measuring system with a dichroic beam splitter. It was tested in a clinical proton field and proven to be applicable up to approx. R_{70} of the Bragg curve.

The results suggest that this method can be used to deliver accurate dosimetry in the region of high dose application, i.e. the height of the Bragg peak, with a remaining dose underestimation in the tail. The measuring system allows for great spatial resolution due to the very small sensitive volume ($0.79\,\mathrm{mm}^3$) of beryllium oxide, which can be made visible within the fiber via x-ray scans. Additionally, it is possible to derive the beam profile from a single irradiation, if the radiation field is created via pencil beam scanning. Furthermore, through the analysis of the γ-factor corresponding to the spectral composition of radioluminescence light in BeO, it is possible to estimate the residual proton range at a given beam quality. The data implies that this is possible in the last 10 mm prior to R_{70} with an accuracy of 1 mm.

The here presented technique can measure several important beam qualities at once with a single probe in a simple and robust way. It is therefore a promising technique to improve and simplify the quality assurance in hadron therapy.

In future research, verification measurements with clinical proton beams are necessary to confirm the accuracy of dose measurements and quantify the remaining dose underestimation.

2022 JINST 17 P02009

References

[1] O.J. Brace, S.F. Alhujaili, J.R. Paino, D.J. Butler, D. Wilkinson, B.M. Oborn et al., *Evaluation of the PTW microDiamond in edge-on orientation for dosimetry in small fields*, *J. Appl. Clin. Med. Phys.* **21** (2020) 278.

[2] Y. Akino, M. Fujiwara, K. Okamura, H. Shiomi, H. Mizuno, F. Isohashi et al., *Characterization of a microSilicon diode detector for small-field photon beam dosimetry*, *J. Radiat. Res.* **61** (2020) 410.

[3] M.A. Schmidt and G.S. Payne, *Radiotherapy planning using MRI*, *Phys. Med. Biol.* **60** (2015) R323.

[4] C. Kirkby, T. Stanescu, S. Rathee, M. Carlone, B. Murray and B.G. Fallone, *Patient dosimetry for hybrid MRI-radiotherapy systems*, *Med. Phys.* **35** (2008) 1019.

[5] T. Teichmann, M. G. Torres, M. van Goethem, E. van der Graaf, J. Henniger, A. Jahn et al., *Dose and dose rate measurements in proton beams using the luminescence of beryllium oxide*, 2018 *JINST* **13** P10015.

[6] L.F. Nascimento, D. Verellen, J. Goossens, L. Struelens, F. Vanhavere, P. Leblans et al., *Two-dimensional real-time quality assurance dosimetry system using* μ*-Al2O3:C,Mg radioluminescence films*, *Phys. Imag. Radiat. Oncol.* **16** (2020) 26.

[7] A.M.C. Santos, M. Mohammadi, J. Asp, T.M. Monro and S. Afshar V., *Characterisation of a real-time fibre-coupled beryllium oxide (BeO) luminescence dosimeter in x-ray beams*, *Radiat. Meas.* **53-54** (2013) 1.

[8] T. Teichmann, J. Sponner, C. Jakobi and J. Henniger, *Real time dose rate measurements with fiber optic probes based on the RL and OSL of beryllium oxide*, *Radiat. Meas.* **90** (2016) 201.

[9] A. Oresegun, Z.H. Tarif, L. Ghassan, H. Zin, H.A. Abdul-Rashid and D. Bradley, *Radioluminescence of cylindrical and flat ge-doped silica optical fibers for real-time dosimetry applications*, *Appl. Radiat. Isot.* **176** (2021) 109812.

[10] A. Oresegun, A. Basaif, Z.H. Tarif, H. Abdul-Rashid, S.A. Hashim and D. Bradley, *Radioluminescence of silica optical fibre scintillators for real-time industrial radiation dosimetry*, *Radiat. Phys. Chem.* **188** (2021) 109684.

[11] E.G. Yukihara, *Luminescence properties of BeO optically stimulated luminescence (OSL) detectors*, *Radiat. Meas.* **46** (2011) 580.

[12] M. Sommer, R. Freudenberg and J. Henniger, *New aspects of a BeO-based optically stimulated luminescence dosimeter*, *Radiat. Meas.* **42** (2007) 617.

[13] M. Sommer, A. Jahn and J. Henniger, *Beryllium oxide as optically stimulated luminescence dosimeter*, *Radiat. Meas.* **43** (2008) 353.

[14] E. Bulur and H. Göksu, *OSL from BeO ceramics: new observations from an old material*, *Radiat. Meas.* **29** (1998) 639.

[15] T. Teichmann, M.J. Gonzalez Torres, K. Makarevich, S. Polter, P. Lachmann, E.R. van der Graaf et al., *Combined OSL-RL measurements for dosimetry in mixed LET proton fields*, in proceedings of the *IEEE Nuclear Science Symposium and Medical Imaging Conference (NSS/MIC)*, Manchester, U.K., 29 October–2 November 2019, pp. 1–3.

[16] G. Erfurt and M.R. Krbetschek, *A radioluminescence study of spectral and dose characteristics of common luminophors*, *Radiat. Prot. Meas.* **100** (2002) 403.

2022 JINST 17 P02009

[17] M. Berger, J. Coursey, M. Zucker and J. Chang, *ESTAR, PSTAR, and ASTAR: Computer Programs for Calculating Stopping-Power and Range Tables for Electrons, Protons, and Helium Ions (version 1.2.3)*, http://physics.nist.gov/Star (2005).

[18] M. Boschini, P. Rancoita and M. Tacconi, *SR-NIEL Calculator: Screened Relativistic (SR) Treatment for Calculating the Displacement Damage and Nuclear Stopping Powers for Electrons, Protons, Light- and Heavy- Ions in Materials (version 7.5.2)*, INFN sezione Milano-Bicocca, Italy, http://www.sr-niel.org/ (2014).

[19] T. Bortfeld, *An analytical approximation of the bragg curve for therapeutic proton beams*, *Med. Phys.* **24** (1997) 2024.

[20] A.S. Beddar, T.R. Mackie and F.H. Attix, *Water-equivalent plastic scintillation detectors for high-energy beam dosimetry: I. physical characteristics and theoretical considerations*, *Phys. Med. Biol.* **37** (1992) 1883.

[21] A.S. Beddar, T.R. Mackie and F.H. Attix, *Water-equivalent plastic scintillation detectors for high-energy beam dosimetry: II. properties and measurements*, *Phys. Med. Biol.* **37** (1992) 1901.

2022 JINST 17 P02009